American Journal of Materials Science and Engineering, 2013, Vol. 1, No. 1, 6-11
Available online at http://pubs.sciepub.com/ajmse/1/1/1

DOI:10.12691/ajmse-1-1-1

Preparation of Alumina-Iron Oxide Compounds by Coprecipitation Method and Its Characterization

Fahmida Gulshan[1,*], Kiyoshi Okada[2]

[1]Materials and Metallurgical Engineering Department, Bangladesh University of Engineering and Technology, Dhaka, Bangladesh
[2]Materials and Structures Laboratory, AMDII Division, Tokyo Institute of Technology, Tokyo, Japan
*Corresponding author: fahmidagulshan@mme.buet.ac.bd

Received January 10, 2013; Revised February 21, 2013; Accepted March 15, 2013

Abstract Fe_2O_3-Al_2O_3 compounds with different Fe/Al compositions were synthesized by coprecipitation (CP) method and calcined at 300 ~1000 ℃. The formation of crystalline phases (e.g., maghemite, hematite), transformation temperature, specific surface area, lattice parameter, crystallite size, magnetic properties of iron oxide were all affected by the component ratio and thermal treatment.

Keywords: *Fe_2O_3-Al_2O_3 compounds, coprecipitation, maghemite, hematite, lattice parameter, crystallite size*

1. Introduction

Mixed oxides, especially binary systems, have been employed successfully in many industrial catalytic processes. The combination of two transitional metal oxides may affect their stoichiometry and their surface, electrical, catalytic, texture and thermal properties. Both Al_2O_3 and Fe_2O_3 individually catalyse many reactions. Binary catalysts with the composition Al_2O_3-Fe_2O_3 are also used for many purposes [1,2].

At present, there are some uncertainties concerning the formation of solid solution in the Fe_2O_3-Al_2O_3 system. The lattice constants at 25 ℃, in terms of trigonal axes for α-Al_2O_3 are: a = 0.4758 and c = 1.2991nm, and those for α-Fe_2O_3 are a = 0.5034 and c = 1.3752nm. The differences in the a and c constants, 5.80 and 5.86%, respectively, are a consequence of different ionic radii of the metals (for coordination six): 0.054nm for Al^{3+} and 0.065nm for Fe^{3+}. Brown et al [3] measured the lattice constants and recorded the Mossbauer spectra for α-Al_2O_3 samples containing Fe^{3+} ions. A linear increase of the constant a with increase of Fe_2O_3 up to 10.5 mol% was observed. A series of aluminium substituted hematites, α-$(Al_xFe_{1-x})_2O_3$ with x up to 0.32, was prepared by Grave et al [4] by thermal treatment of aluminium substituted goethites, α-FeOOH, at 500 ℃ for 6h. The samples contained particles varying in size from 20 to 100nm, as determined from X-ray diffraction line broadening. Heating of the samples up to 900 ℃ improved the crystallinity, but reduced the maximum obtainable x to ~0.15. Mossbauer spectroscopy was applied for quantitative determination of aluminium substituted goethite-hematite mixtures by Amarasiriwardena et al [5]. The effects of crystallinity and aluminium substitution on the magnetic behaviour and Morin transition of these substituted oxides were also investigated [6,7] and found that aluminium substituted hematite, prepared under hydrothermal conditions from coprecipitated Al(III)/Fe(III)-hydroxides at temperatures not high enough to remove OH^- structural groups, exhibited a substantial deviation from the Vegard rule. The anhydrous aluminium substituted hematites, treated at 900 ℃, fulfilled the Vegard rule in the solid solution range ($x \leq 0.15$). The ball milling of equimolar mixtures of goethite and hydrated aluminas, γ-$Al(OH)_3$ (gibbsite), α-$Al(OH)_3$ (bayerite) or γ-AlOOH (boehmite) significantly affected the temperature of formation of solid solution of the calcined products [8].

The aim of the present study was to obtain more detailed knowledge about the formation of solid solutions in an analogous system Fe_2O_3-Al_2O_3. The effect of component ratio and thermal treatment conditions on the phase composition and structure were investigated. The samples synthesized were used to test their effectiveness for adsorption of toxic ions in waste-water followed by the magnetic separation by applying a simple magnetic field. The study of this system is of particular interest in connection with the polymorphs of its components and possible phase conversions, which can be followed by X-ray diffraction methods for both components and magnetochemistry of phases containing iron.

2. Experimental

2.1. Synthesis Procedures of Fe_2O_3-Al_2O_3 Compound by Coprecipitation Method

The coprecipitation process involves dissolving a salt precursor, usually a chloride, oxychloride or nitrate. The corresponding metal hydroxides precipitate in water upon addition of a base solution such as sodium hydroxide or ammonium hydroxide solution. The resulting salts are then washed and calcined to obtain the final oxide powder. This method is useful in preparing ceramic composites of different oxides by coprecipitation of the corresponding hydroxides in the same solution. One disadvantage of this

method resides in the difficulty in controlling the particle size and size distribution.

In this study, ferric nitrate $Fe(NO_3)_3.9H_2O$ and aluminium nitrate $Al(NO_3)_3.9H_20$ were used as precursors of Fe_2O_3 and Al_2O_3 to prepare Fe_2O_3-Al_2O_3 compound. Coprecipitated gels were prepared with various ratios of 0.2M $Fe(NO_3)_3{\cdot}9H_2O$ and $Al(NO_3)_3{\cdot}9H_2O$ solutions using conc. NH_4OH (25 mass%) as the precipitant. Samples containing 0, 20, 40, 60, 80 and 100 mol% Fe_2O_3 were prepared. For example, to prepare 20 mol% Fe_2O_3 sample, 4.04g $Fe(NO_3)_3{\cdot}9H_2O$ was dissolved in 50 ml of distilled water and 15.01g $Al(NO_3)_3{\cdot}9H_2O$ was dissolved in 200ml of distilled water. Then, these two solutions were mixed with mechanical stirring and 200ml of NH_4OH solution was added with continuous stirring. They were dried in an evaporator at 60 ℃ for 4h and in an oven at 110 ℃ for 2 days.

2.2. High Energy Ball Milling

After drying, the powders were dry-ground in a planetary ball mill (LAPO-1, Ito Seisakusho Ltd., Japan) using a Si_3N_4 pot with 30 Si_3N_4 balls (5 mmϕ) at 300rpm for 3 hours with a ball: sample mass ratio of 30:1. In this process, known as 'break down' or 'top-down' approach, high mechanical grinding energy is applied to produce nanoparticles.

2.3. Calcination

After grinding, the samples were calcined at 300 °- 1000 ℃ in air for 5 hours at a heating rate of 10 ℃ /min. The flowchart for the preparation of the sample is shown in Figure 1.

2.4. Characterization of Samples

The crystalline phases in the samples were determined by x-ray diffraction analysis (XRD-6100, Shimadzu) using monochromated CuKα radiation. The lattice parameters of the resulting crystalline phases were calculated by least-squares method using Si powder as the internal standard. The crystallite sizes of the crystalline phases were calculated using the Scherrer equation for the (104) reflection of α-Fe_2O_3 and α-Al_2O_3, and the (400) of γ-Al_2O_3. The instrumental broadening was corrected using the peak widths measured for 100 mol% Fe_2O_3 sample heated at 1300 ℃. The specific surface area (S_{BET}) was obtained by the multipoint BET method using N_2 as the adsorbate (Autosorb-1, Quantachrome). The magnetic properties were examined using vibrating sample magnetization (VSM) equipment (BHV-50H, Riken Electronics).

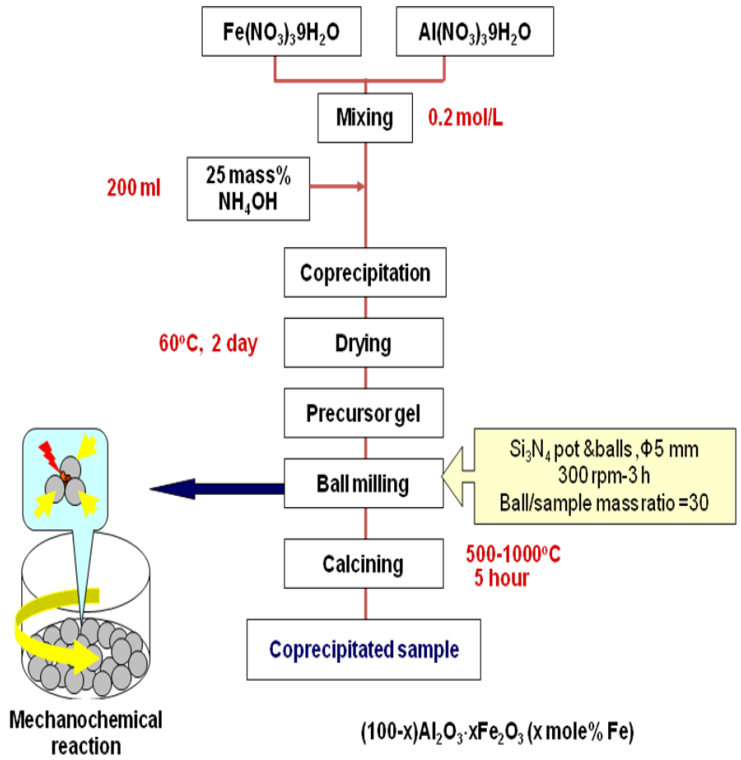

Figure 1. Flowchart for the preparation of Al_2O_3-Fe_2O_3 compounds by coprecipitation method

3. Results and Discussion

3.1. Characterization of Samples

The x-ray diffraction patterns of the samples calcined at various temperatures are shown in Figure 2 (a-e). From these figures it is clear that the as-synthesized samples were amorphous, but crystallized at 500-700 ℃ in all samples. The crystallization temperature increased with increasing Al_2O_3 content in the Fe-rich compositions, being highest at about 60 mol% Fe_2O_3 composition. In the Fe-rich compositions, the crystalline phase was α-Fe_2O_3 and was thought to incorporate Al_2O_3. The increase of iron content in the CP samples is associated with an increase of intensities of the α-Fe_2O_3 reflections, therefore with higher crystallinity of the phase. In the Al-rich compositions, the crystalline phases changed from γ-Al_2O_3 to θ-Al_2O_3 and then to α-Al_2O_3 at higher temperatures

In the 20 mol% Fe_2O_3 sample (Figure 3), the only detectable phase at temperature 600 ℃ is γ-Al_2O_3, located at 2θ= 36.95, 45.46, 66.36°. At temperature 800 ℃, the XRD pattern shows the appearance of new XRD reflections at 2θ = 24.15, 33.25, 35.72, 49.65, 54.30, 62.68 and 64.28^0 are attributed to α-Fe_2O_3. The intensity of the latter XRD reflections strongly increased with the increase of calcination temperature indicating the enhancement of crystallinity of α-Fe_2O_3. A phase transition of γ-Al_2O_3 to α-Al_2O_3 is clearly observed upon elevating the calcination temperatures to 1000 ℃.

A field map of the product phases as functions of composition and heating temperature is shown in Figure 4. From this field map, it can be seen that the formation of α-Fe_2O_3 takes place at 600 ℃ in 80 mol% Fe_2O_3 samples and 700 ℃ in 60 mol% Fe_2O_3 whereas α-Fe_2O_3 is formed at 500 ℃ in 90 mol% Fe_2O_3 sample. The crystallization of α-Fe_2O_3 shifted gradually to higher temperature by increasing the alumina content, indicating the effect of alumina.

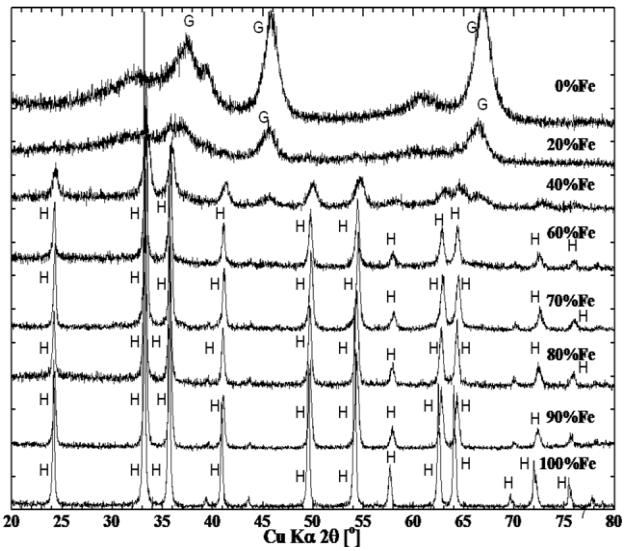

Figure 2(c). The XRD pattern of the samples heated at 700 ℃ for different Fe/(Fe+Al) ratio. Key: G = γ-Al_2O_3, H = α-Fe_2O_3

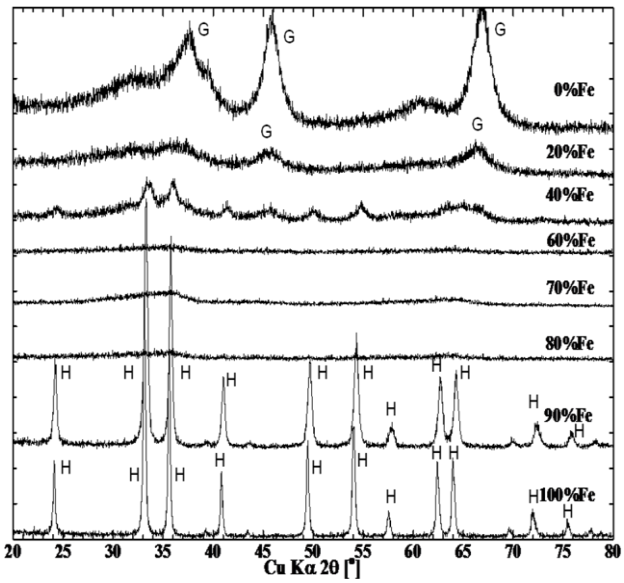

Figure 2(a). The XRD pattern of the samples heated at 500 ℃ for different Fe/(Fe+Al) ratio. Key: G = γ-Al_2O_3, H = α-Fe_2O_3

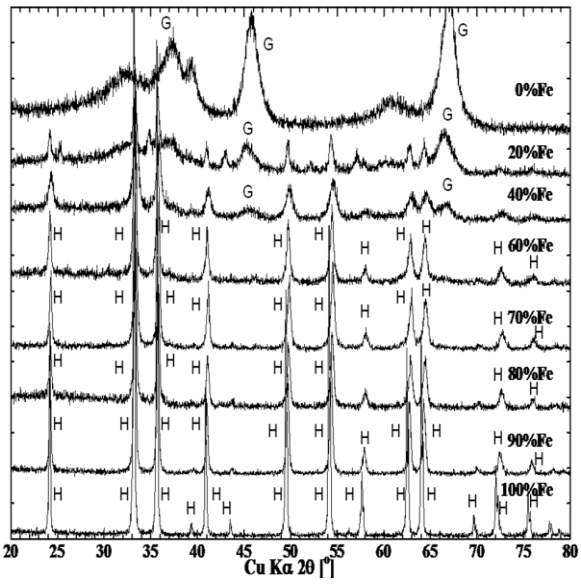

Figure 2(d). The XRD pattern of the samples heated at 800 ℃ for different Fe/(Fe+Al) ratio. Key: G = γ-Al_2O_3, H = α-Fe_2O_3

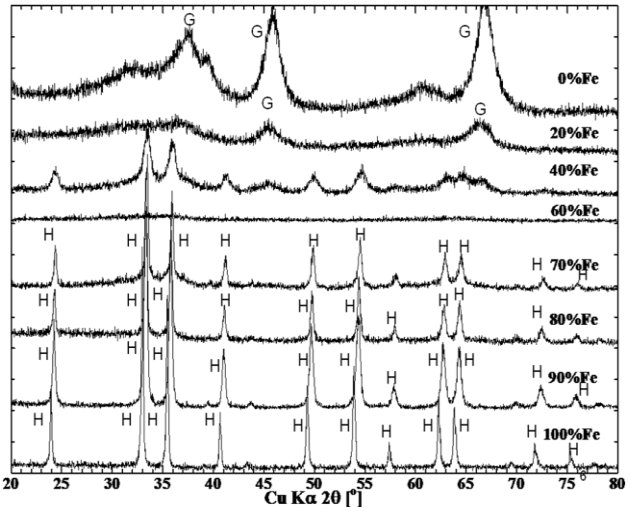

Figure 2(b). The XRD pattern of the samples heated at 600 ℃ for different Fe/(Fe+Al) ratio. Key: G = γ-Al_2O_3, H = α-Fe_2O_3

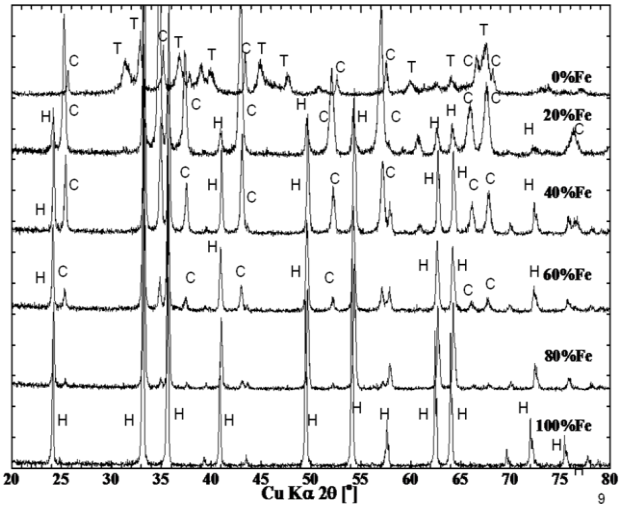

Figure 2(e). The XRD pattern of the samples heated at 1000 ℃ for different Fe/(Fe+Al) ratio. Key: C = α-Al_2O_3, H = α-Fe_2O_3,T=θ-Al_2O_3

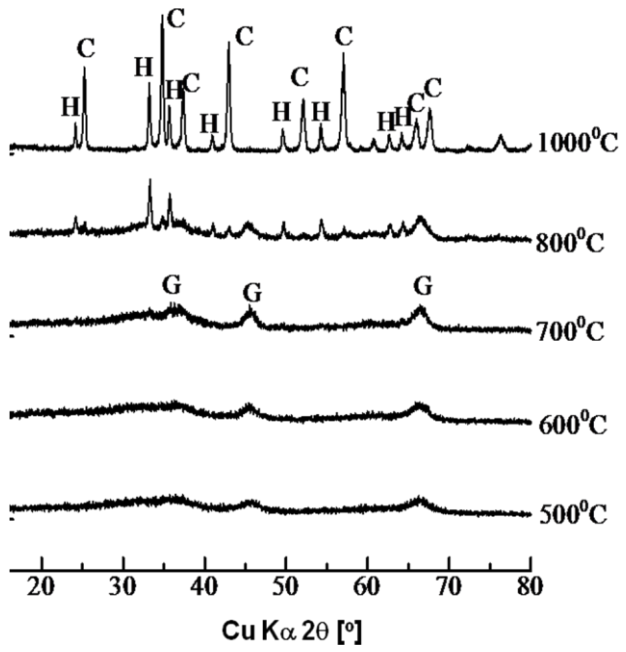

Figure 3. The XRD patterns of the 20 mol% Fe_2O_3 CP samples heated at different calcination temperatures. Key: C = α-Al_2O_3, G = γ-Al_2O_3, H = α-Fe_2O_3

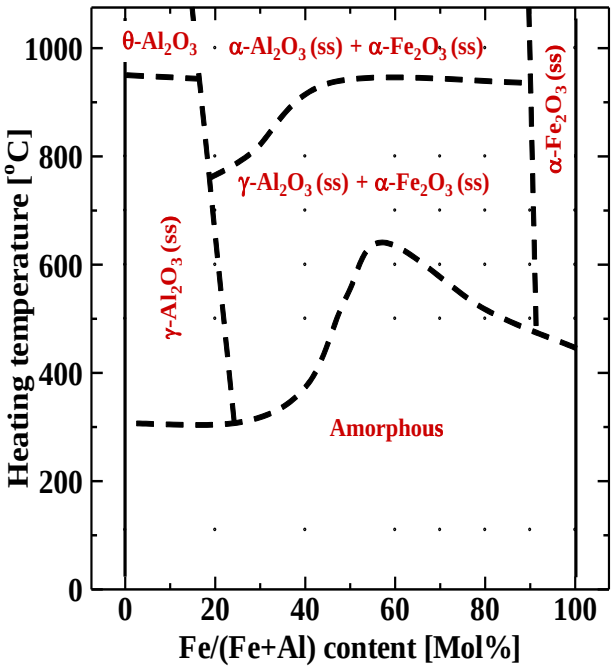

Figure 4. A field map of the phases formed in the samples as functions of composition and calcined temperature

Table 1. Lattice constants (nm) of α-Fe_2O_3 in the various samples

Temp[℃]		Fe/(Fe + Al) [mol%]				
		20	40	60	80	100
500	*a*		0.4961(8)*			0.50388(9)
	c		1.3630(62)			1.3768(7)
600	*a*		0.49941(9)		0.50135(4)	0.50498(30)
	c		1.3641(6)		1.3678(3)	1.3815(23)
700	*a*		0.49970(43)	0.50107(11)	0.50150(13)	0.50327(2)
	c		1.3579(32)	1.3672(9)	1.3691(10)	1.3737(2)
800	*a*	0.50167(15)	0.50008(12)	0.50113(22)	0.50090(14)	0.50344(1)
	c	1.3702(12)	1.3642(9)	1.3675(17)	1.3667(11)	1.37360(6)
1000	*a*	0.5009(30)	0.50177(4)	0.50237(19)	0.50172(9)	0.50368(4)
	c	1.378(23)	1.3682(3)	1.3713(15)	1.36848(7)	1.3748(3)

* The numbers in the parentheses represent the standard deviation in the last decimal places
Reference data α-Al2O3: a=0.4758, c=1.2991 [ICDD No.10-0173]; α-Fe2O3: a=5.0356, c=13.7489[ICDD No. 33-064]

The lattice parameters of the Fe-rich samples (Table 1) decreased with decreasing Fe_2O_3 content up to 40 mol% Fe_2O_3 in samples heated at ≤800 ℃. The amount of Al_2O_3 estimated from the resulting lattice parameters was about 20 mol% in these samples. By contrast, the lattice parameters of the samples heated at 1000 ℃ decreased in samples containing up to 90 mol% but became constant in the samples containing ≤90 mol% Fe_2O_3. The limit of Al_2O_3 incorporation in these samples is found to be ≤10 mol%, in fair agreement with Pownceby et al. [9]. Thus, the resulting data observed at ≤800 ℃ appear to correspond to a transient state that attains equilibrium on heating at ≥1000 ℃.

The lattice parameters determined for Al-rich samples suggest that 10-20 mol% of Fe_2O_3 is incorporated in the γ-Al_2O_3 and α-Al_2O_3 phases.

Thus, the crystalline phases in the samples of intermediate compositions are solid solutions of Fe_2O_3 and Al_2O_3. The incorporation of Al or Fe ions in these phases causes broadening of their XRD reflections, suggesting smaller crystallite sizes. The crystallite sizes of the samples [showed in Figure 5] were estimated using the Scherrer's equation, $D = K\lambda/\beta\cos\theta$, where D is the crystallite size, λ is the X-ray wavelength (0.15418nm), K is a numerical constant (0.9), β is the full width at half maximum for the reflection and θ is the Bragg angle [10].The crystallite sizes of the α-Fe_2O_3 in 100 mol% Fe_2O_3 samples varied from 73nm at 500 ℃ to 460nm at 1000 ℃ while those of the 40 mol% Fe_2O_3 samples ranged from 9.1nm at 500 ℃ to 140nm at 1000 ℃. Thus, the crystallite sizes of the pure Fe_2O_3 samples are several times larger than those of the Al_2O_3-containing samples. The crystallite sizes of the α-Al_2O_3 samples decreased from 150nm in the 20 mol% Fe_2O_3 sample to 71nm in the 40 mol% Fe_2O_3 sample. The crystallite sizes of γ-Al_2O_3 also decreased with higher Fe_2O_3 content, from 5.8nm at 500 ℃ to 6.1nm at 800 ℃ in the 0 mol% Fe_2O_3 and from 3.4nm at 500 ℃ to 5.3nm at 800 ℃ in the 40 mol% Fe_2O_3 sample.

3.2. Magnetic Properties

The magnetic properties of the samples were measured to determine their potential usefulness for magnetic separation after adsorption. The magnetization was determined as a function of magnetic field at room temperature by VSM. It employs an electromagnet which provides the magnetizing field (DC), a vibrator mechanism to vibrate the sample in the magnetic field, and detection coils which generate the signal voltage due to the changing flux emanating from the vibrating sample.

The output measurement displays the magnetic moment (*M)* as a function of the magnetic field (*H)*. This applied magnetic field was varied from -15000 Oe to 15000 Oe. All the samples showed very weak saturation magnetization, <1emu/g.

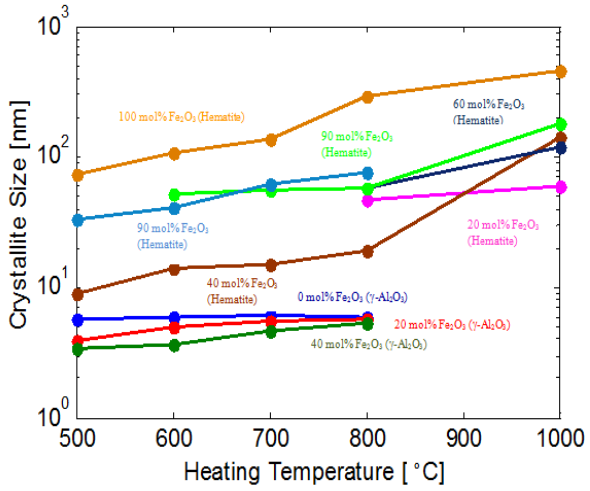

Figure 5. Crystallite size vs. temperature as a function of Fe/(Fe+Al)

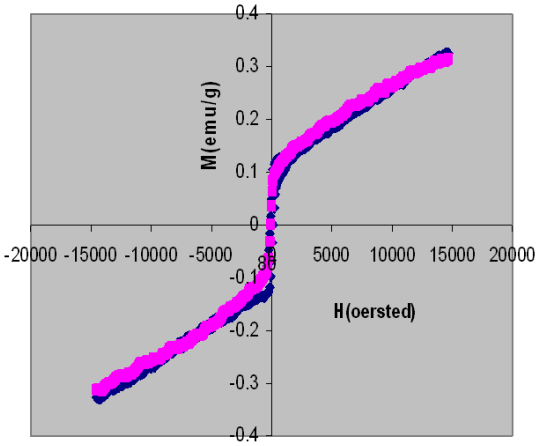

Figure 6. Magnetization curves of 80 mol% Fe_2O_3 CP sample calcined at 800 ℃ [blue line] and that at 1000 ℃ [pink line]

The samples containing α-Fe_2O_3 solid solutions showed very weak hysteresis loops in the magnetization curves [Figure 6] corresponding to the antiferromagnetic property of α-Fe_2O_3 and the magnetization was insufficient to attract these powders to a domestic magnet.

3.3. Specific Surface Area

Changes in the S_{BET} values of the samples of various compositions [values listed in Table 2] are shown in Figure 7 as a function of heating temperature and Fe_2O_3 content, together with the values reported by Li et al. [11]. The S_{BET} values differed greatly, ranging from 330m^2/g in the sample with 0 mol% Fe_2O_3 heated at 500 ℃ to 3m^2/g in the sample containing 100 mol% Fe_2O_3 heated at 800 ℃. The S_{BET} values decreased slightly with higher heating temperature to 1000 ℃. On the other hand, the effect of the Fe_2O_3 content on S_{BET} was different in the samples with Fe_2O_3≤80 mol% and Fe_2O_3=100 mol%. The S_{BET} values were almost constant or slightly less, up to Fe_2O_3≤80 mol% contents, but decreased very steeply from 80 to 100 mol%. Figure 6 suggests that mixtures of crystalline phases are effective in maintaining high S_{BET} values. The S_{BET} values of the present samples (solid lines) are higher than those reported by Li et al. [11] (dashed lines).

Table 2. Specific surface area values [m^2/g]

Fe/(Fe+Al) [Mol%]	Calcination temperature [℃]			
	500 ℃	600 ℃	700 ℃	800 ℃
0	331	283	229	155
20	262	238	197	85
40	211	148	90	69
60	225	134	72	38
80	191	62	37	27
100	14	8	5	3

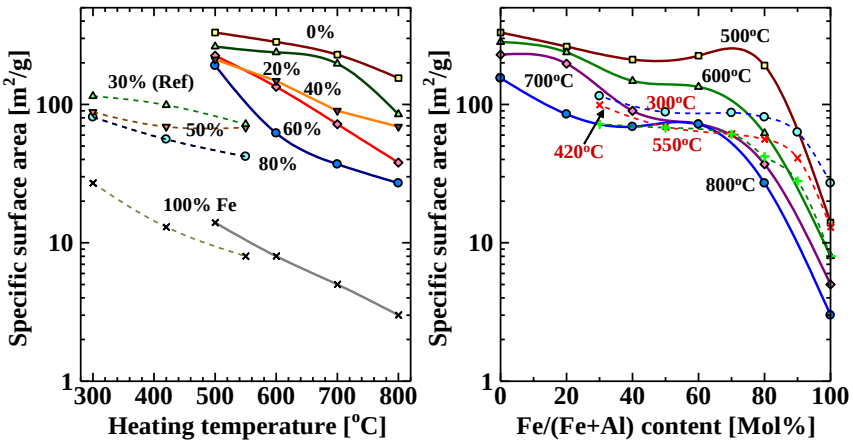

Figure 7. Changes in the S_{BET} values of the samples of various compositions as a function of heating temperature and Fe_2O_3 content, together with the values reported by Li et al[11]

4. Conclusion

The as-synthesized samples were amorphous but crystallized on heating at 500-700 ℃. The crystalline phases formed were only α-Fe_2O_3 in the Fe-rich compositions, while they ranged from γ-Al_2O_3 to θ-Al_2O_3 to α-Al_2O_3 with increasing heating temperature in the Al-rich compositions. About 10-20mol% of Al_2O_3 was incorporated in α-Fe_2O_3 and a similar amount of Fe_2O_3

was incorporated in γ-Al_2O_3 and α-Al_2O_3. The crystallite sizes decreased significantly by incorporation of these ions. The S_{BET} values differed greatly from $330m^2/g$ to $3m^2/g$. The samples showed very weak magnetization.

References

[1] Lee, E. H. "Iron Oxide Catalysts for Dehydrogenation of Ethylbenzene in the Presence of Steam", *Catalysis Reviews*, 8(1). 285.1974.

[2] Lee, E. H. and Oliver, G. D., "Calculating Homogeneous Reaction Rates and Orders in a Flowing Gas Reactor. Thermal Decomposition of Ethylbenzene", *Ind. Eng. Chem.*, 1959, 51 (11). 1351-1352. November .1959.

[3] Brown,I. W. M., Mackenzie, K. J. D. and Cardile,C. M., "Lattice parameters and Mössbauer spectra of iron-containing corundum (α-Al2O3)", *Journal of Materials Science Letters*, 6(5).535-540. May .1987.

[4] Grave,E.De., Bowen, L.H. and Weed, S.B., "Mossbauer Study Of Aluminum-Substituted Hematites", *Journal of Magnetism and Magnetic Materials*, 27(1). 98-108. 1982.

[5] Amarasiriwardena,D.D., Grave, E.De. and Bowen L.H., "Quantitative Determination of Aluminum-Substituted Goethite-Hematite Mixtures by Mössbauer Spectroscopy", *Clays and Clay Minerals*, 34(3). 250-256. June .1986.

[6] Grave, E.De., Bowen, L.H., Vochten, R. and Vandenberghe,R.E., "The effect of crystallinity and Al substitution on the magnetic structure and morin transition in hematite", *Journal of Magnetism and Magnetic Materials*, 72(2), 141-151. April. 1988.

[7] Wolska, E. and Szajda, W., "The effect of cationic and anionic substitution on the α-(Al, $Fe)_2O_3$ lattice parameters", *Solid State Ionics*, 28 (2). 1320-1323. September. 1988.

[8] Tsuchida, T. and Sugimoto,K., "Effect of grinding of mixtures of goethite and hydrated alumina on the formation of Fe_2O_3-Al_2O_3 solid solutions", *Thermochim. Acta*, 170. 41-50.1990.

[9] Pownceby,M.I., Constanti-Carey, K.K. and Fisher-White, M.J., "Subsolidus Phase Relationships in the System Fe2O3-Al2O3-TiO2 between 1000° and 1300°C", *Journal of the American Ceramic Society*, 86(6). 975-980. June. 2003.

[10] Nedelec, J.M,. Avignant, D. and Mahiou, R., "Soft chemistry routes to YPO4-based phosphors: dependence of textural and optical properties on synthesis pathways", *Chemistry of materials*, 14 (2). 651-655. 2002.

[11] Li, F.B., Li, X.Z., Liu, C.S. and Liu, T.X., "Effect of alumina on the photocatalytic activity of iron oxides for bisphenolA degradation", *J. Hazard. Mater*. 149. 199-207. 2007.